Structure of an Interleukin-1β Mutant with Reduced Bioactivity Shows Multiple Subtle Changes in Conformation That Affect Protein–Protein Recognition[†,‡]

Nancy P. Camacho,[§,∥,⊥] Deborah R. Smith,[§,∥] Adrian Goldman,[§,#] Bohdan Schneider,[§,○] David Green,[△] Peter R. Young,[△] and Helen M. Berman*[,§]

Department of Chemistry and the Waksman Institute, Rutgers University, New Brunswick, New Jersey 08903, and Department of Molecular Genetics, SmithKline Beecham Pharmaceuticals, King of Prussia, Pennsylvania 19406-0939

Received April 6, 1993; Revised Manuscript Received May 21, 1993

ABSTRACT: Site-specific mutagenesis was used to obtain the human interleukin-1β mutant protein with glycine substituted for threonine at position 9 (IL-1β Thr9Gly). The mutant maintains receptor binding but exhibits significantly reduced biological activity. The crystal structure of IL-1β Thr9Gly has been determined at 2.4-Å resolution by molecular replacement techniques and refined to a crystallographic *R*-factor of 19.0%. IL-1β Thr9Gly crystallizes in a different space group ($P6_522$) than does native IL-1β ($P4_3$); thus the molecules pack differently. Their overall structure is similar, nevertheless, with both composed of 153 amino acids which form 12 antiparallel β-strands. However, significant conformational differences both close to and far from the site of the mutation may explain the mutant's altered properties.

IL-1α and IL-1β are two structurally related proteins that mediate a range of biological activities involved in immunological and inflammatory responses in many tissues and cell types (Dinarello, 1991). They exert their effects by binding to receptors on the surface of the target cell (Curtis *et al.*, 1989; Sims *et al.*, 1988). A third related protein, IL-1ra, binds to the same receptors but has no biological activity (Arend, 1991). It therefore appears that two regions of IL-1 are required for activity—one to bind the receptor and the second to stimulate a biological response. However, because of the low amino acid identity between IL-1 molecules (Clore & Gronenborn, 1991; Clore *et al.*, 1991; Eisenberg *et al.*, 1991; Finzel *et al.*, 1989; Graves *et al.*, 1990; Priestle *et al.*, 1988; Stockman *et al.*, 1992; Veerapandian *et al.*, 1992; Young & Sylvester, 1989) and the fact that most of the conserved or identical residues are not on the surface (Priestle *et al.*, 1989), examination of the known X-ray crystallographic and/or multidimensional NMR structures of these three proteins does not provide sufficient information to identify precisely which residues bind the receptor and which stimulate a biological response.

Several mutagenesis studies have begun to elucidate key residues which affect both these events. These include mutations which alter both receptor binding and biological activity, suggesting that they primarily affect regions required for receptor binding (Huang *et al.*, 1987; Kamogashira *et al.*, 1988; Labriola-Tompkins *et al.*, 1991; MacDonald *et al.*, 1986). Other mutations appear to have no effect on receptor binding but significantly reduce biological activity, implying that they affect regions involved in receptor signal transduction (Gehrke *et al.*, 1990; Ju *et al.*, 1991; Simon *et al.*, 1993). As the latter mutations are at residues quite distant from each other rather than localized on one face of IL-1β, it is unclear how they lead to the same end result. There has, however, been an attempt to address this issue in one mutant via modeling (Auron *et al.*, 1992).

We report here the crystal structure of an IL-1β mutant prepared by replacement of threonine 9 with glycine (Thr9Gly). Thr9Gly exhibits receptor affinity comparable to that of IL-1β but does not elicit biological activity (Simon *et al.*, 1993). We find that differences between wild-type IL-1β and Thr9Gly are not just localized to the region of the mutation.

EXPERIMENTAL PROCEDURES

The protein purification was as previously described (Simon *et al.*, 1993). The protein was stored in 150 mM NH_4OAc, pH 5.2, at a concentration of 4.4 mg/mL and was dialyzed into 50 mM PIPES, pH 7.0, immediately prior to each crystallization setup.

IL-1β Thr9Gly was crystallized at room temperature from 10 μL of hanging drops which contained an initial protein concentration of 3.4 mg/mL and 0.168 M ammonium sulfate. The drops were sealed and allowed to equilibrate over a 1-mL bath of 2.1 M ammonium sulfate for 3–5 weeks.

Two data sets were collected, designated set 1 and set 2. Set 1 was collected from a single, colorless crystal measuring 0.7 mm × 0.5 mm × 0.15 mm. Set 2 was collected from a single, colorless crystal measuring 0.8 mm × 0.4 mm × 0.12 mm. Diffraction data were collected to 2.5 Å for set 1 and to 2.4 Å for set 2, both at 0 °C on a Xuong–Hamlin Mark II electronic area detector system (San Diego Multiwire Systems) mounted on a Rigaku RU-200 rotating anode X-ray generator (Cu Kα radiation). The anode was operated at 50 kV and 100 mA. The crystal was rotated about the ω axis and 0.1° oscillation frames were collected. Data reduction was performed with UCSD Multiwire software (Xuong *et al.*, 1985) as follows: oscillation frames were scaled together and merged using a single scale factor per 5° ω-wedge per detector. The scale factors were refined to minimize the discrepancy between

[†] This research was supported by a grant from the NIH (GM 21589-19). Support for D.R.S. was provided by Molecular Biophysics Training Grant NIH GM08319 and in part by a grant from the Pittsburgh Supercomputing Center funded through the NIH and NSF.

[‡] The crystallographic coordinates have been deposited in the Brookhaven Protein Data Bank under the file name 1HIB.

* Author to whom correspondence should be addressed.

[§] Rutgers University.

[∥] These authors made equal contributions to the work reported here.

[⊥] Current address: The Hospital for Special Surgery, 535 E. 70th St., New York, NY 10021.

[#] Current address: Center for Biotechnology, IF-20521 Turku, Finland.

[○] Current address: Heyrovsky Institute, Czech Academy of Sciences, 18223 Prague, Czech Republic.

[△] SmithKline Beecham Pharmaceuticals.

0006-2960/93/0432-8749$04.00/0

Table I: Summary of Crystallographic Analysis of Thr9Gly

crystal data		
contents of asymmetic unit		
molecules of Thr9Gly		1 monomer of Thr9Gly
mol wt		17400
unit cell dimensions		
a (Å)		55.43(1)
b (Å)		55.43(1)
c (Å)		241.94(6)
α (deg)		90.00
β (deg)		90.00
γ (deg)		120.00
space group		$P6_522$
V_m (Å^3/Da)		3.1
data collection	**data set 1**	**data set 2**
crystal size (mm)	0.8 × 0.5 × 0.15	0.8 × 0.4 × 0.12
temp (°C)	0	0
crystal mounting	capillary	capillary
data collection device	Xuong–Hamlin Mark II electronic area detector	Xuong–Hamlin Mark II electronic area detector
radiation	Cu Kα, λ = 1.5418 Å; Rigaku RU-200 rotating anode	Cu Kα, λ = 1.5418 Å; Rigaku RU-200 rotating anode
resolution range (Å)	∞ to 2.4	∞ to 2.27
reflections		
measured	38975	30094
unique: $F > 0\sigma(F)$	7593	8534
unique: $F > 2\sigma(F)$	7344	8159
data coverage (%)[a]	90	90
R_{sym}	0.046	0.062
structure determination (data set 1)		
molecular replacement		
rotation solution	peak ratios (peak 1/peak 2)	
	1.49 (residues 31–153)	
	1.19 (residues 3–153)	
translation solution		
$z = 1/2$	2.03 (residues 3–153)	1.30 (residues 31–153)
$y = 0$	1.29 (residues 3–153)	1.17 (residues 31–153)
$x = 0$	1.50 (residues 3–153)	1.37 (residues 31–153)
refinement (data set 2)		
resolution (Å)		10.0–2.4
residues		3–153
no. of solvent molecules		113
R-factor (%)[b]		19.0
reflections: $F > 2\sigma(F)$		8143
rms deviations[c]		
distances (Å)		
bond		0.017/0.020
bond angle		0.046/0.040
dihedral angle		0.035/0.035
peptide planes (Å)		0.012/0.020
chiral volumes (Å^3)		0.221/0.200
nonbonded contacts (Å)		
single torsion		0.169/0.200
multiple torsion		0.188/0.200
possible H-bonds		0.129/0.200

[a] Data coverage refers to the number of unique structure factor observations divided by the number of structure factor observations possible. [b] $R = \sum(F_o - F_c)/\sum(F_o)$, where F = structure factor amplitude, F_o = observed (measured) F, and F_c = calculated F. [c] The left number gives the rms deviations from ideal values in the final model, and the right number is the target σ used in the final stage of refinement.

observations of the symmetry-related reflections in different wedges, and outliers were automatically rejected. Three rounds of scaling and rejection were performed before the data were finally merged (See Table I for statistics).

During preliminary data collection it was determined that the crystal had hexagonal symmetry, and data were collected assuming a Laue symmetry of $6/m$. After data reduction, it was evident, on the basis of both equivalent and systematically absent reflections, that the space group was either $P6_122$ or $P6_522$. Data were then processed in space group $P622$ (Table I). Cell dimensions were $a = b = 55.43(1)$ Å and $c = 241.94(6)$ Å, with one molecule per asymmetric unit.

The structure of IL-1β Thr9Gly was determined by molecular replacement using the Crowther rotation function (Crowther, 1972) and the Crowther and Blow translation function (Crowther & Blow, 1967) as implemented in the package MERLOT (Fitzgerald, 1988, 1991). Two models were used: the native IL-1β protein including residues 3–153, as well as the same model without the N-terminus (Table I) (Finzel *et al.*, 1989; Protein Data Bank code 1I1B).

For the rotation function, the model was placed in a triclinic orthogonal cell with dimensions $a = b = c = 125$ Å and inverse Fourier-transformed. The resulting structure factors were used in rotations against the observed Thr9Gly data from set 1. Data between 8.0- and 4.0-Å resolution were used. An unambiguous solution was obtained for the full as well as the truncated model.

The rotated model was then used as input to the translation search. For both space groups $P6_122$ and $P6_522$, the translation function was sampled approximately every 1.0 Å along u, v and w and 8.0–4.0 Å data were used with origin removal. A set of internally consistent vectors from three Harker sections was found for space group $P6_522$ (but not for $P6_122$) (Table 1). The rotated, translated model was then refined in this space group, as described below.

The resultant model was refined using XPLOR (Brunger, 1990). The initial R-factor ($R = \Sigma|F_o - F_c|/\Sigma F_o$, where F_o and F_c are the observed and calculated structure factors, respectively) of 53.0% dropped to 28.5% after one round of simulated annealing refinement utilizing 6.0–2.8-Å data with $F/\sigma(F) > 2$. After each cycle of refinement F_o, $F_o - F_c$, and $2F_o - F_c$ electron density maps were prepared and displayed with the molecular graphics program FRODO (Jones, 1978) on an Evans and Sutherland PS390 graphics system. Insertions and adjustments of residues were made and the new coordinates refined.

The $2F_o - F_c$ maps prepared after the first round of refinement revealed that residues 3–8 and 150–153 were not in density. These residues were deleted from the model for the next round of refinement and were only added as the refinement progressed. The $F_o - F_c$ map (σ level of 3.0) was used to locate solvent molecules, 113 of which have been found to date. Water molecules were positioned only where a discrete sphere of electron density was situated within 2.5–3.3 Å of a hydrogen bond donor or acceptor. Solvent molecules were considered acceptable if following refinement their B-values were comparable to those of the neighboring regions of Thr9Gly.

Upon the addition of solvent molecules the R-factor dropped from 21.4% to 19.1%, employing a cutoff of $F/\sigma(F) > 4$ for 6.0–2.5-Å data from set 1. In the last stage of refinement with XPLOR, 10.0–2.4-Å data from set 2 were used with a cutoff of $F/\sigma(F) > 2$. The resulting R-factor was 19.3%. Following XPLOR refinement, the root-mean-square (rms) deviation from ideality for bond lengths was 0.017 Å, 4.2° for bond angles, and 3.5° for chirality of the peptide bond.

Following minor adjustments, PROLSQ (Hendrickson & Konnert, 1981) was used for the final round of coordinate refinement, employing the same data set and limits imposed in the previous step. Upon convergence the final R-factor for

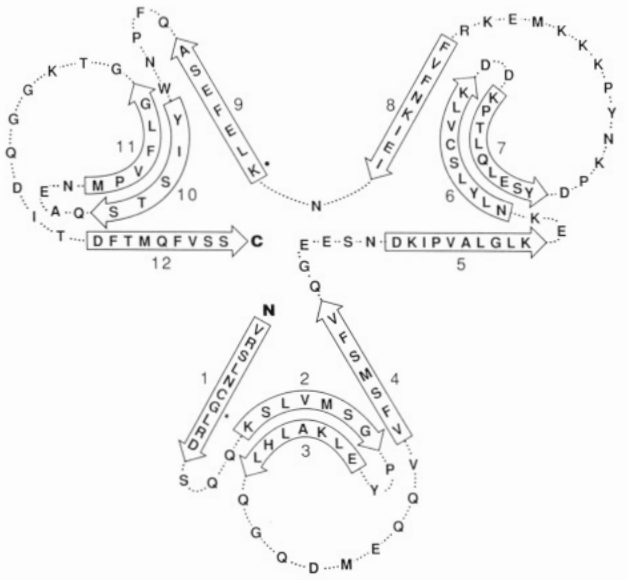

FIGURE 1: Schematic showing correlation between secondary structure and amino acid sequence of Thr9Gly [format based on diagram by Priestle *et al.*, (1988)].

8143 reflections above 2σ in the resolution range 10.0–2.4 Å was 19.0%. Considering all 8526 reflections from 20.0 to 2.4 Å, the final *R*-factor was 22.9%. The rms deviation for bond angles following PROLSQ refinement was 2.7 and 2.4° for the peptide bond. Statistics for the refinement are shown in Table I.

Using data set 1, the loop between β3 and β4 proved very difficult to fit; however, this problem was largely resolved through the use of data set 2. Nevertheless, there were still some small areas of the molecule which exhibited ambiguous electron density. These included residues 34–35, residues 53–54, and the side chains of residues 93–94. As there was sufficient density to position the side chains, these coordinates have been included; however, the reliability of these regions must be considered questionable. The latter region was also difficult to fit in the wild-type IL-1β structure. Additionally, there was insufficient density in the 107–108 region to place both residues, so asparagine 107 has been deleted from the coordinate list. As with two of the wild-type IL-1β molecules whose structures were determined (Finzel *et al.*, 1989, PDB code 1I1B; Veerapandian, 1992, PDB code 4I1B), no density could be found for the first two residues. Coordinates and structure factors have been deposited with the Brookhaven Protein Data Bank.

RESULTS

Molecular Overview. Both wild-type IL-1β and the Thr9Gly molecule consist of 12 antiparallel β-strands (Figure 1, Table II) with no α-helices; the principal feature is a six-stranded β-barrel composed of β1, β4, β5, β8, β9, and β12 (Figure 2). While wild-type IL-1β has two stretches of 3_{10} helix (from residues 33 to 39 and from residues 96 to 98) as defined by the parameters of Kabsch and Sander (Laskowski *et al.*, 1992; Morris *et al.*, 1992), only the latter region forms a 3_{10} helix in Thr9Gly.

Like the parent IL-1β molecule and its structural twin, the Kunitz soybean trypsin inhibitor (Blow *et al.*, 1974; Sweet *et al.*, 1974), Thr9Gly exhibits approximately 3-fold internal symmetry consisting of a repeating βββLβ motif, where L is a large loop. It is interesting to note that, in the first β-strand of the repeating motifs, the amino acid which corresponds to the Thr9Gly position invariably possesses a β-carbon.

Table II: Nomenclature for Topology in IL-1β and IL-1β Thr9Gly[a]

β-strands	IL-1β residues	IL-1β Thr9Gly residues
β1	3–12	3–12
β2	17–21	16–22
β3	25–29	25–31
β4	40–52	41–47
β5	55–62	54–63
β6	66–74	66–74
β7	77–85	77–85
β8	100–106	99–106
β9	109–114	109–115
β10	120–125	121–125
β11	130–125	130–135
β12	142–152	145–153
β-turns	**IL-1β residues**	**IL-1β Thr9Gly residues**
T1	12–15	13–15
T2	21–24	23–24
T3	33–36 (3_{10} helix)	32–40 (T3*)
T4	34–37	
T5	35–38	
T6	52–55	48–53
T7	62–65	64–65
T8	74–77	75–76
T9	86–89	86–94
3_{10} helix	96–98	96–98
T10	106–109	108
T11	114–117	116–119
T12	117–120	117–120
T13	126–129	126–129
T14	136–141	146–144

[a] Secondary structure assignment made by PROCHECK (Laskowski *et al.*, 1992; Morris *et al.*, 1992).

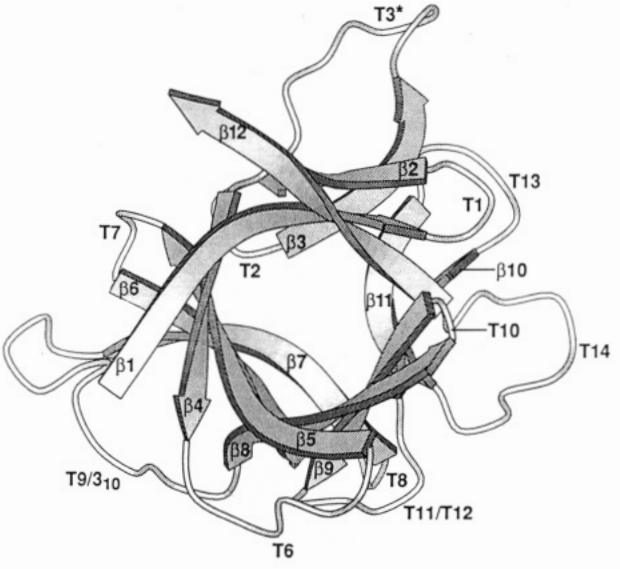

FIGURE 2: Richardson diagram (Richardson, 1981) of the Thr9Gly backbone with turns and β-strands numbered. The figure was drawn using the program MOLSCRIPT (Kraulis, 1991).

A best molecular fit (BMF) (Nyburg, 1974) comparison of the wild-type and Thr9Gly structures employing all α-carbons except for that of Asn107 gives a root-mean-square (rms) deviation of 1.43 Å. When all loops are removed from both structures except for residues 32–40, the rms deviation actually increases to 1.51 Å. Upon removal of the 32–40 loop region from both sequences, the rms deviation drops to 1.00 Å.

Secondary Structure. The various structural features of Thr9Gly and the three available wild-type IL-1β structures (Brookhaven Protein Data Bank entries 1I1B, Finzel *et al.*, 1989; 2I1B, Priestle *et al.*, 1988; 4I1B, Veerapandian, 1992) were evaluated using PROCHECK (Laskowski *et al.*, 1992; Morris *et al.*, 1992). As illustrated by the Ramachandran

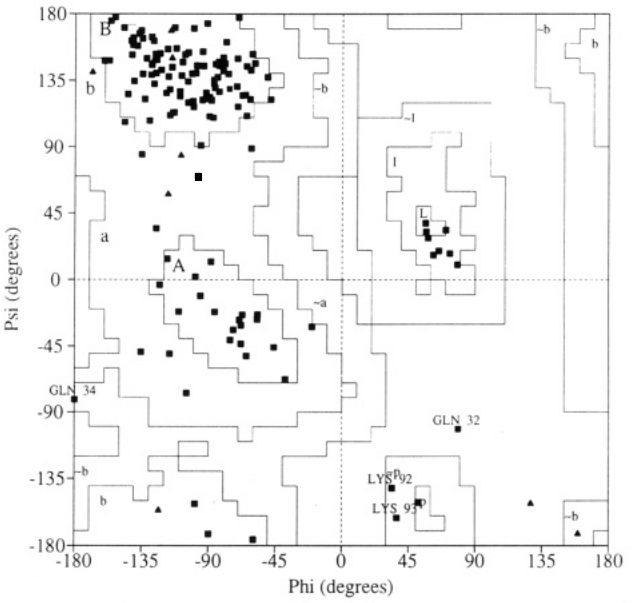

Plot statistics

Residues in most favoured regions [A,B,L]	105	80.8%
Residues in additional allowed regions [a,b,l,p]	21	16.2%
Residues in generously allowed regions [~a,~b,~l,~p]	3	2.3%
Residues in disallowed regions	1	0.8%
Number of non-glycine and non-proline residues	130	100.0%
Number of end-residues	4	
Number of glycine residues (shown as triangles)	9	
Number of proline residues	7	
Total number of residues	150	

Based on an analysis of 118 structures of resolution of at least 2.0 Angstroms and R-factor no greater than 20%, a good quality model would be expected to have over 90% in the most favoured regions.

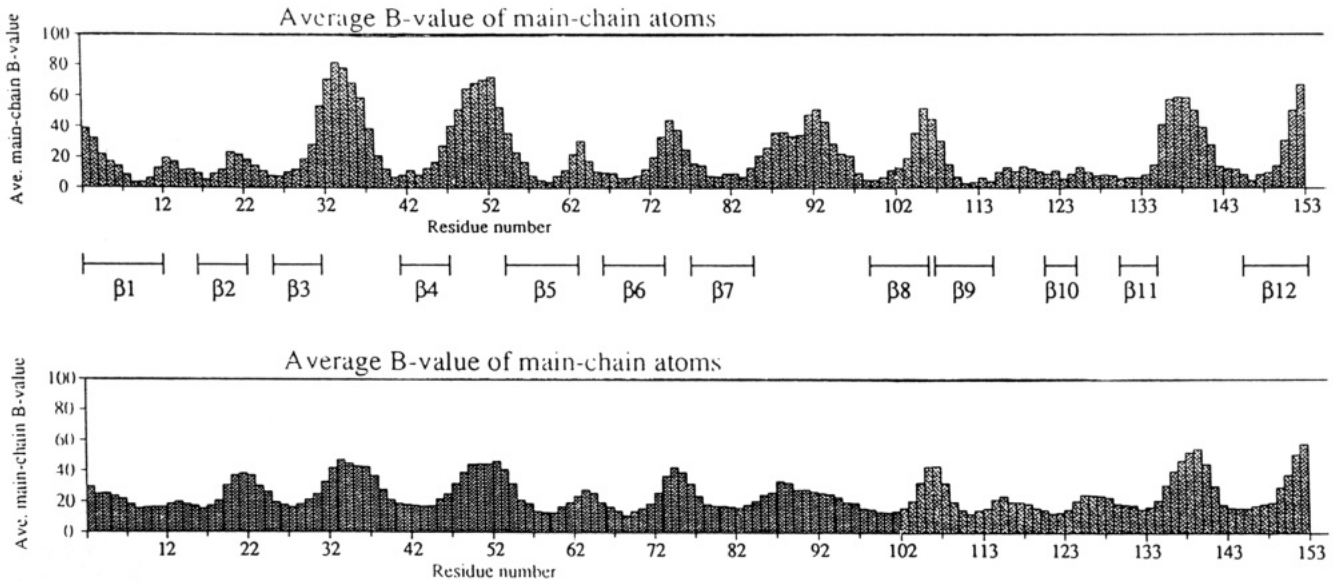

FIGURE 3: Selected structural features prepared using the program PROCHECK (Laskowski *et al.*, 1992; Morris *et al.*, 1992). (a, top) Ramachandran plot for comparison with other structures. ϕ vs Ψ (degrees) for main-chain atoms of Thr9Gly, following refinement with PROLSQ. Residues in generously allowed and disallowed regions are labeled. (b, bottom) Comparison between Thr9Gly (top) and wild-type IL-1β (bottom) (Finzel *et al.*, 1989) of the temperature factor distribution as a function of sequence, with β-strands of Thr9Gly labeled. Numbering is sequential as per the residues present in the Thr9Gly structure, i.e., 3–106, 108–153.

plot (Figure 3a), Thr9Gly has one residue in the disallowed region and three in the generously allowed regions. While all three wild-type structures also have residues in these disfavored regions, there is considerable variation with regard to the amino acids affected. For example, in 1I1B (Finzel *et al.*, 1989), residue 108 is in a generously allowed and residue 141 in a disallowed region. In contrast, 2I1B (Priestle *et al.*, 1988) has only two of 153 amino acids within the generously allowed regions, namely Pro2 and Asn107, while 4I1B has Asp75 and Asn107 as well as Gln141 in generously allowed regions (data not shown).

Similarly, in plots of χ_1 vsχ_2, no side chains of Thr9Gly are more than 2.5 standard deviations from the ideal, while residues 20, 54, 75, 102, and 119 of 1I1B show significant deviations in the values of χ_2 (data not shown). As with the ϕ,Ψ plots of the three wild-type proteins, the χ_1 vs χ_2 plots of 2I1B and 4I1B demonstrate considerable disparity with regard to the side chains involved and the degree of deviation from the norm.

As with all three wild-type IL-1β structures, Thr9Gly has a *cis* peptide bond between Tyr90 and Pro91. Although hydrogen bonds between side chains in the region that precedes the 3_{10} helix of Thr9Gly apparently serve as anchors through

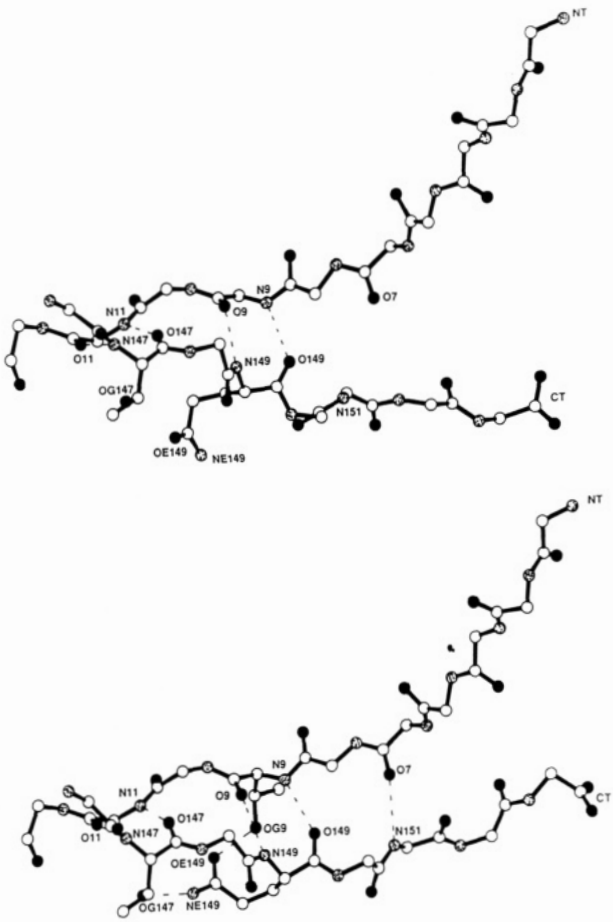

FIGURE 4: Comparison of Thr9Gly and wild-type IL-1β at the mutation site: Thr9Gly (top); wild-type (bottom) (Finzel *et al.*, 1989). Nitrogen atoms are stippled, oxygen atoms are shaded, and the remaining atoms are open. Atoms involved in hydrogen bonds in the wild-type protein are labeled in both structures. Figures were prepared using the program DOCK (Stodola *et al.*, 1988).

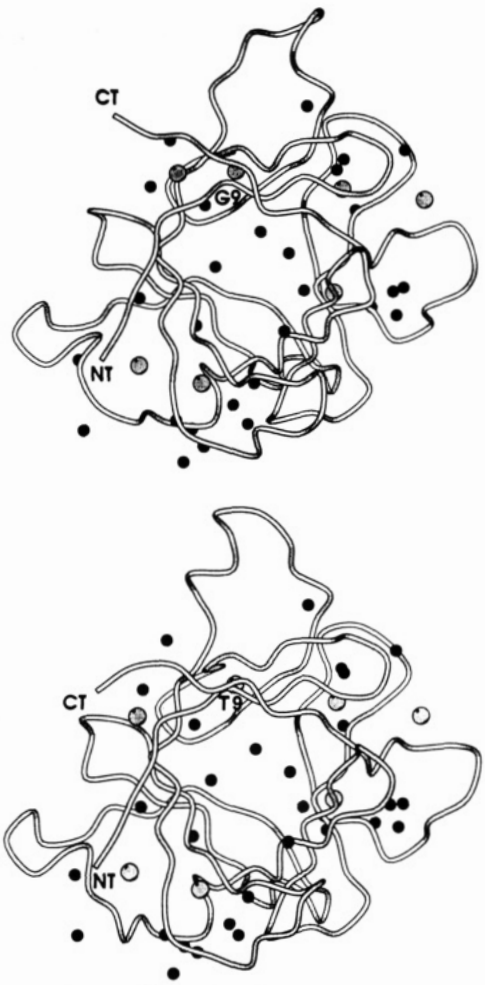

FIGURE 5: Diagram illustrating the water molecules common to both structures. Larger solvent molecules depict waters defined as "internally bound" by Finzel *et al.*, (1989) including that water near the C-terminus which is not superimposable but is in a comparable position in Thr9Gly. Figures were prepared using the program MOLSCRIPT (Kraulis, 1991). Thr9Gly (top); wild-type IL-1β (bottom) (Finzel *et al.*, 1989).

which the *cis* conformation is stabilized, the actual hydrogen bonds employed differ somewhat from those found in the wild-type protein. While in wild-type IL-1β hydrogen bonds link the carboxylate group of Glu96 to the side chains of Tyr90 and Lys92 (Finzel *et al.*, 1989), in Thr9Gly the Glu96 carboxylate group forms hydrogen bonds with the side chains of both Tyr90 and Lys93.

β-turns were categorized according to the scheme of Richardson (1981) (Table II). There is a close correlation in the conformation of all turns in Thr9Gly and wild-type IL-1β, with the exception of the region between residues 32 and 40. We have nevertheless called this region T3* to be consistent with the nomenclature used for the wild-type molecule.

Intramolecular contacts were evaluated (Carrell, 1979). In general, if the distance between nitrogen and oxygen atoms was between 2.5 and 3.2 Å, they were considered to be potential hydrogen-bonding pairs. Of the 88 hydrogen bonds in Thr9Gly, only 4 are near the extremes of these limits. Without exception, these are located either within turns connecting β-strands or at the ends of the β-strands.

One of the potential side-chain to side chain hydrogen bonds found only in the wild-type molecule involves the γ-hydroxyl of Thr9. This and the ϵ-carboxyl of Gln149 form a hydrogen bond, while the ϵ-amino group of Gln149 forms a hydrogen bond with the γ-hydroxyl of Thr147 (Figure 4). Consequently, two hydrogen bonds stabilize this region in the wild-type protein, and their presence or absence is undoubtedly responsible for the markedly different conformations exhibited by side-chain 149 in the two structures (Figure 4 ; see also Figure 8). In addition, wild-type IL-1β possesses two more hydrogen bonds—one involving a water molecule—which serve to stabilize contacts between the protein's amino and carboxy termini. Notably, the loss of these hydrogen bonds would appear to be responsible for the greater divergence between the termini of Thr9Gly (Figures 4 and 5).

Other hydrogen bonds unique to the wild-type protein encompass three residues of β9 which bridge remote regions of the primary sequence. While two of these contacts are replaced by hydrogen bonds to water molecules in Thr9Gly, the third involves an interaction between the side chains of Glu111 and Lys138, which is in close proximity to Asp145. It is interesting to note that, like Thr9Gly, Asp145Lys mutants of IL-1β retain the capacity to bind the receptor without eliciting a biological response. As expected, the wild-type protein exhibits a markedly different hydrogen-bonding pattern in the T3* loop which permits the formation of the 3_{10} helix in that molecule.

Thr9Gly possesses unique hydrogen bonds, one of which involves the O10 of β1 and the N18 of β2. Although this bond is immediately adjacent to the mutation site, its significance is not readily apparent. The only other noteworthy hydrogen bond which is unique to Thr9Gly is one between N47 of β4 and O57 of β5.

Atomic Mobility. As shown in Figure 3b, the general trend for the temperature factors is such that the β-pleated sheets

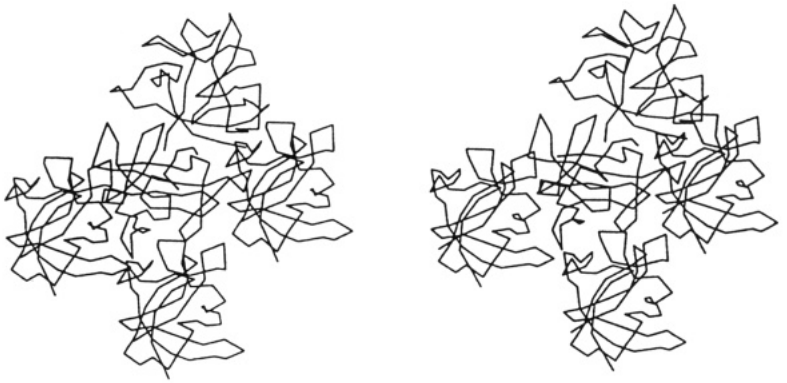

FIGURE 6: Stereoview of the packing of Thr9Gly α-carbons in the crystal. The figure was drawn using the program DOCK (Stodola *et al.*, 1988).

and turns that pack against other molecules have low temperature factors, while turns such as T9 that are not involved in hydrogen-bonding interactions have higher temperature factors. The only exception to this is the T3* region which although involved in intermolecular contacts still appears to have higher temperature factors. This may be due to the possibility that it has alternative conformations which we were unable to model.

Crystal Packing. Because Thr9Gly crystallizes in a hexagonal space group ($P6522$) as opposed to the tetragonal space group ($P4_3$) of wild-type IL-1β, the two molecules necessarily exhibit different packing geometries. Although both proteins pack against four neighboring molecules (Figure 6), where the wild-type molecule rests at the center of a relatively equilateral tetrahedron, Thr9Gly occupies the center of a noticeably flattened tetrahedron, with molecules at each apex.

For Thr9Gly, three distinct intermolecular contacts are involved. In the first the N- and C-terminal regions, as well as T10, interact with the C- and N-terminal regions and T10 of the symmetry-related molecule along one of the 2-fold axes. The second involves contacts by T6, T8, T12, T14, and the area of 3_{10} helix of Thr9Gly, interacting with the corresponding face of the symmetry-related molecule. The third contact is between the Thr9Gly face comprised of T1/β2, β3/T3*, and T13, which interacts with a symmetry-related surface consisting of T2, β7/T9, and T7/β6. The inverse of this interaction makes up the tetrahedron. A schematic comparing packing geometries and interactions between the wild-type and mutant proteins is shown in Figure 7.

When Thr9Gly is placed in the $P4_3$ space group of the parent molecule sterically unfavorable contacts result, especially in the β3/T3* and T7/β6 regions, while β7/T9, T11, and T8 as well as both termini exhibit considerably fewer forbidden contacts. Similarly, there are unfavorable contacts when the wild-type structure is placed in the $P6_522$ cell. Most notably these involve steric hindrance between T13 and the β6/T9 regions and the carboxy termini of neighboring molecules. Additional unlikely contacts exist between β3 and the T2/β7 areas and between the second portion of 3_{10} helix and T8, as well as between T10s of adjacent proteins.

It is likely that some of the structural differences between Thr9Gly and wild-type IL-1β are due to packing constraints. For example, side chains of Arg4, His30, Glu128, and Phe150 adopt different orientations in the two molecules (Figure 8), and all four of these side chains are involved in different types of packing interactions in the different crystals. In the wild-type molecule the side chain of Arg4 is hydrogen bonded to the side chain of Glu113, as well as to the carbonyl group of Ser114, while in Thr9Gly this residue forms a hydrogen bond

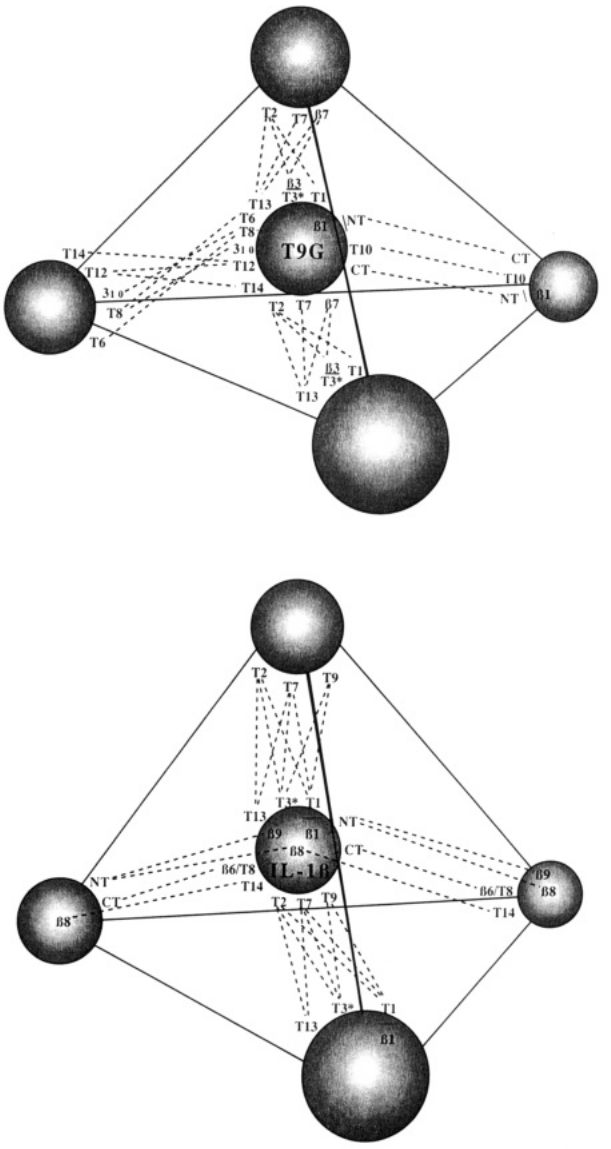

FIGURE 7: Schematic comparing the packing interactions of the two structures. T = turn/loop region; β = β-strand; T9G = Thr9Gly; dotted lines connect the regions of secondary structure involved in contacts between symmetry-related molecules. Those β-strands which are part of the β-barrel and which contain residues involved in packing interactions are denoted by being placed directly on the circles representing the molecules.

with the carbonyl of Val151. Likewise, Glu128 of Thr9Gly forms a hydrogen bond with the side chains of Tyr24 and Ser84, where the wild-type counterpart forms a hydrogen bond with the side chain of Lys65. In Thr9Gly, Phe150 is encased in a "pocket" formed by hydrophobic side chains of a nearby

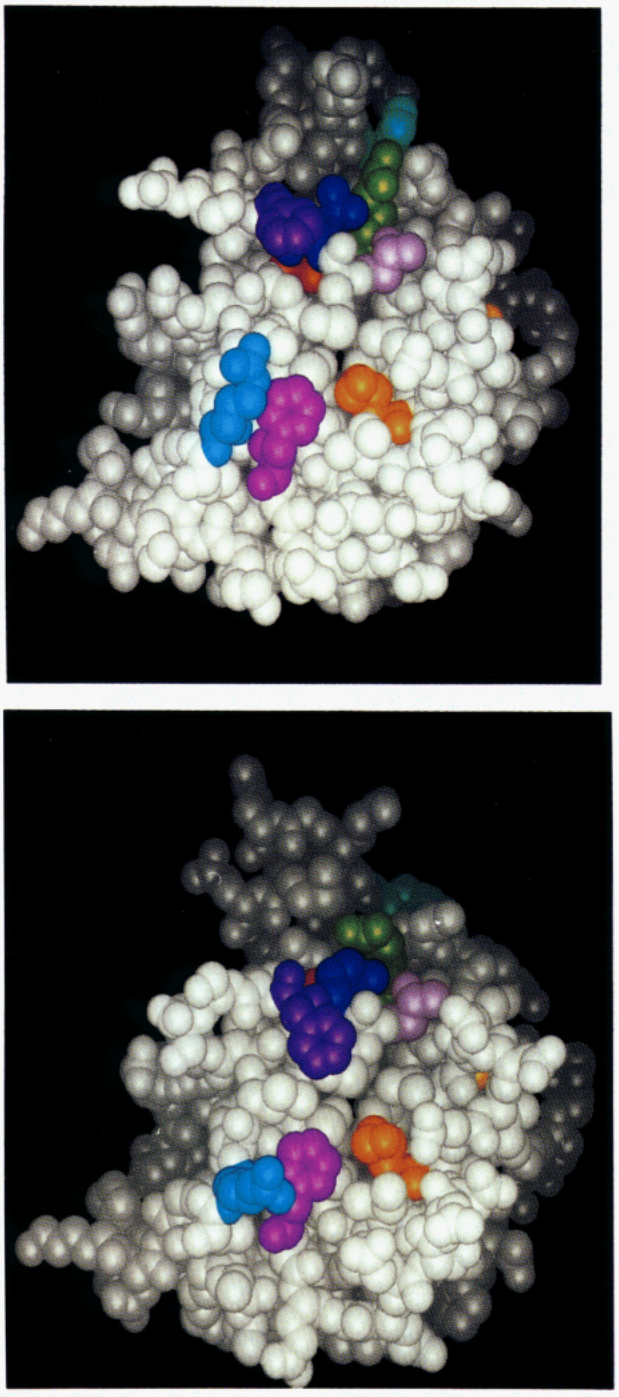

FIGURE 8: Comparison of space-filling models (INSIGHTII, 1992) looking down the open end of the β-barrel: (a, top) Thr9Gly; (b, bottom) wild-type IL-1β (Finzel *et al.*, 1989). Residues are color-coded as follows: Arg4 (medium blue, lower left), residue forms hydrogen bond with symmetry-related molecule in both proteins. Gly9/Thr9 (red, upper middle), side chain of wild-type residue is involved in hydrogen bonds with Thr147 and Gln149. Arg11 (light green, upper right), residue is involved in intramolecular hydrogen bonds in Thr9Gly and forms a hydrogen bond with water in the wild type. His30 (light blue, upper right), ring is involved in intermolecular stacking in Thr9Gly and in intermolecular hydrogen bonds in the wild type. Phe46 (magenta, lower left), ring is not involved in packing or hydrogen bonds in either molecule. Lys103 (orange, lower right), residue is not involved in packing or hydrogen bonds in either structure. Gln145 (yellow, middle right), residue forms hydrogen bond with water in Thr9Gly and is involved in intramolecular hydrogen bond in the wild type. Thr147 (lavender, upper right), side chain forms hydrogen bond with water in Thr9Gly and with side chain of Thr9 in the wild type. Gln149 (dark blue, upper center), residue forms hydrogen bonds with two water molecules in Thr9Gly and is involved in intramolecular hydrogen bond in the wild type. Phe150 (violet, upper left), residue is involved in packing in both molecules, although to a much greater extent in Thr9Gly.

symmetry-related molecule which constrains the orientation of the phenyl ring, while in wild-type IL-1β the interactions involving this residue are far less extensive and restrictive. In wild-type IL-1β, His30 forms an intermolecular hydrogen bond with a symmetry-related molecule, whereas His30 of Thr9Gly is not involved in any intermolecular hydrogen bonds. Instead, its imidazole ring stacks with the Tyr24 side chain of an adjacent molecule.

Solvent Structure. Of the 113 waters placed in Thr9Gly, 35 occupy essentially identical positions in both proteins. Superimposing Thr9Gly and the wild-type structures (Finzel *et al.*, 1989), there are 12 waters within 0.5 Å, another 12 within 0.75 Å, and an additional 11 within 1.0 Å of one another in the two proteins. Seven of the eight water molecules found bound in the interior of wild-type IL-1β are also found in Thr9Gly. Of these, three are located within 0.5 Å, one within 0.75 Å, and two within 1.0 Å of their wild-type counterparts. The seventh water, while residing 5.0 Å from the corresponding wild-type residue, is situated between residues 7 and 151 of the N- and C-termini. Thus, while these two waters are not superimposable, they occupy roughly comparable positions within the molecule and are involved in similar contacts with the adjacent residues (Figure 5). The only internally bound water not found in Thr9Gly is one of the waters bridging the gap between residues 10 and 40. Waters not exposed on the surface which were hydrogen bonded to the protein were considered to be internally bound, and Thr9Gly possesses 13 such water molecules. The wild-type molecule has 8 such water molecules (Finzel *et al.*, 1989).

Interactions with solvent may also play a role in conformational changes of some of the side chains. For example, Gln145 and Gln149 of Thr9Gly form hydrogen bonds with solvent molecules, while the corresponding residues of the wild-type molecule hydrogen bond to the side chains of Ser13 and Thr9/Thr147, respectively. Likewise, Arg11 of the wild-type protein forms hydrogen bonds with water, while in Thr9Gly it forms a hydrogen bond with the side chain of Gln15.

DISCUSSION

IL-1β binds to a target cell surface receptor and in so doing elicits a biological response in the target cell. How the binding event triggers responses inside the target cell is not understood, although the most plausible models involve interaction of the IL-1β–receptor complex with accessory proteins. By analogy to other receptors, this may involve direct contact of IL-1β with the second protein and/or induced conformational changes in the receptor which allow the association to occur, thus leading to biological activity.

Evidence for these models comes from mutagenesis studies of IL-1β which show in a few cases that loss of biological activity is not linked to loss of receptor affinity (Gehrke *et al.*, 1990; Ju *et al.*, 1991; Simon *et al.*, 1993). These mutations can be explained if the mutant IL-1β fails to induce a key conformational change upon receptor binding or lacks the appropriate surface residues to interact with a second cell surface protein. Similar data have been reported for IL-1α and IL-1ra (Ju *et al.*, 1991; Yamayoshi *et al.*, 1990).

Thr9Gly is such a mutant IL-1β. It binds to both human and murine IL-1 type I receptors with an affinity comparable to that of wild-type IL-1β and yet has a biological activity that is reduced approximately 200-fold (Simon *et al.*, 1993). Two other IL-1β mutations fall into this category, Asp145Lys (Ju *et al.*, 1991) and Arg11Gly (Auron *et al.*, 1992; Gehrke *et al.*, 1990). Examination of the wild-type IL-1β structure does not readily explain how these three mutations can have

the same effect, especially since Asp145 is on a different face of IL-1β to Thr9 and Arg11.

This structure reveals that Thr9Gly has essentially the same overall secondary and tertiary structure of wild-type IL-1β. However, there are a number of significant conformational changes. The alteration of Thr9 to Gly results in the local disruption of a hydrogen-bonding interaction between the side chains of Thr9 and Gln149, as well as a backbone hydrogen bond between Asn7 and Val151. This loosens the interaction between the amino- and carboxy-terminal β-strands (strands 1 and 12) and results in a shift in the orientation of the carboxy terminus. There are also significant changes in the loop between residues 32 and 40. The result of these and other more subtle changes is to alter the packing and interaction with adjacent molecules in the crystal lattice. Thus the change from Thr to Gly at residue 9 is not limited to a local conformational change but affects more distal regions of the molecule, and it is the combination of some of these changes which probably causes the altered protein–protein interactions.

Unfortunately, changes in the arrangement of surface residues do not convincingly explain the altered properties of Thr9Gly because many of the more dramatic effects involve residues which interact with symmetry-related molecules in the crystal. This is illustrated by an examination of the face of IL-1β recently proposed to be involved in binding to the type I IL-1 receptor (Figure 8). Five residues (Arg4, His30, Phe46, Lys103, and Thr147) have been implicated in receptor binding (Graves *et al.*, 1990; Huang *et al.*, 1987; Labriola-Tompkins *et al.*, 1991; MacDonald *et al.*, 1986). No changes were observed in Phe46, Lys103, and Thr147, but there are changes in Arg4 and His30. Therefore, one might naively argue that this face of IL-1β cannot be involved in receptor binding because the Thr9Gly mutant does not have altered binding even though the conformations of residues Arg4 and His30 are changed in this mutant. This would be false. The changes in side-chain conformation for Arg4 and His30 are almost certainly due to changed crystal packing contacts; these side chains could easily adopt wild-type or other, as yet unknown, conformations when the Thr9Gly mutant binds to the receptor.

Along these lines, the significant alterations to the carboxy terminus and the 32–40 loop are probably not the explanation of Thr9Gly's altered activity. Deleting the carboxy-terminal four amino acids has no effect on biological activity (Mosley *et al.*, 1987), and mutagenesis of Phe150 to Ala results in only a 2-fold drop in receptor binding (Labriola-Tompkins *et al.*, 1991). Mutagenesis of His30 of human IL-1β (MacDonald *et al.*, 1986) and Gln33 of murine IL-1β (Daumy *et al.*, 1991) results in significant reductions in both receptor binding and biological activity. Furthermore, while this loop is constrained in its conformation in wild-type IL-1β (Finzel *et al.*, 1989), this is almost certainly a result of its interaction with a symmetry-related molecule in the crystal lattice since the 4D NMR of IL-1β indicates that it is in rapid motion (Clore & Gronenborn, 1991). Hence the differences in the apparent conformation of this loop are probably due to the different crystal-dependent molecular interactions.

In contrast to the above, it is clear that the underlying conformation shifts are very real. Indeed, distal changes in conformation were suspected from 2D NMR spectrum comparisons between wild-type IL-1β and Thr9Gly (Simon *et al.*, 1993). Although model building studies on the Arg11Gly mutant suggest that Asp145 might be essential for triggering a biological response (Auron *et al.*, 1992), the conformation of that residue is not markedly changed in Thr9Gly. However, it is perhaps significant that the only internally bound water found in wild-type IL-1β that is absent in Thr9Gly is one of the three waters involved in the hydrated pocket bounded by strands β1, β2, and β4. It has been suggested that these three solvent molecules may provide structural support for the Asp145 region. While Thr9Gly also has alterations in the hydrogen bonding of Arg11 along the lines predicted for the Arg11Gly mutant, including the loss of bound water which is replaced by a hydrogen-bonding interaction with Gln15, this does not seem to be sufficient for a change at Asp145. However, it should be noted that the alteration of Asp145 to Lys also may not be a local change, since it may result in repulsion between Lys145 and Lys109 and/or hydrogen bond formation between Lys138 and Glu111. Clearly, to know which conformational changes occur in all these mutants requires detailed structural information on all of them. Such knowledge is the minimum necessary to understand what changes cause altered receptor binding and what changes cause altered stimulation of biological response. Ultimately, this question may only be answered by determining the structures of IL-1β–receptor complexes.

That the subtle alterations due to the Thr9Gly mutation can lead to significant changes in protein–protein interactions is illustrated by the changes in packing between the wild-type and Thr9Gly structures. Indeed, it may be that the surface regions of IL-1β which interact intermolecularly in the crystal lattice may be the same ones that are involved in IL-1β–receptor interactions. Such is the case with insulin, where Arg22, Gly23, Phe24, Phe25, and Tyr26 comprise the putative receptor binding site (Steiner *et al.*, 1985) and residues 23–26 associate with the same four residues of a symmetry-related molecule across a 2-fold axis (Smith *et al.*, 1982).

These results have implications for other studies where attempts have been made to use mutations in surface residues as a way to identify key protein-protein contacts. If there are no alterations in the overall folding of a particular mutant ligand as determined by antibody recognition or circular dichroism, there is a tendency to conclude that the mutation affects a surface residue directly involved in receptor–ligand interaction. While this approach has been successful in some cases (de Vos *et al.*, 1992), the present study shows that nonlocal changes in conformation can be responsible for the observed effects.

ACKNOWLEDGMENT

We are grateful for the assistance by Mark Eaton and Christopher Wilson, who grew the crystals used in this study. We thank Dick Leidich of the X-ray Facility at the Waksman Institute. We also thank Paula Fitzgerald and Shri C. Jain for their helpful advice.

REFERENCES

Arend, W. P. (1991) *J. Clin. Invest. 88*, 1445–1451.

Auron, P. E., Quigley, G. J., Rosenwasser, L. J., II, & Gehrke, L. (1992) *Biochemistry 31*, 6632–6638.

Blow, D. M., Janin, J., & Sweet, R. M. (1974) *Nature 249*, 54–57.

Brunger, A. T. (1990) *X-PLOR (Version 2.1): A system for crystallography and NMR*, Yale University, New Haven, CT.

Carrell, H. L. (1979) *BANG: A program for the rapid calculation of bond lengths and angles*, The Institute for Cancer Research, The Fox Chase Cancer Center, Philadelphia, PA.

Clore, G. M., & Gronenborn, A. M. (1991) *J. Mol. Biol. 221*, 47–53.

Clore, G. M., Wingfield, P. T., & Gronenborn, A. M. (1991) *Biochemistry 30*, 2315–2323.

Crowther, R. A. (1972) in *The Molecular Replacement Method* (Rossmann, M. G., Ed.) Gordon and Breach, New York.

Crowther, R. A., & Blow, D. M. (1967) *Acta Crystallogr. 23*, 544–548.

Curtis, B. M., Gallis, B., Overell, R. W., McMahan, C. J., DeRoos, P., Ireland, R., Eisenman, J., Dower, S. K., & Sims, J. E. (1989) *Proc. Natl. Acad. Sci. U.S.A. 86*, 3045–3049.

Daumy, G. O., Wilder, C. L., Merenda, J. M., McColl, A. S., Geoghegan, K. F., & Otterness, I. G. (1991) *FEBS Lett. 278*, 98–102.

de Vos, A. M., Ultsch, M., & Kossiakoff, A. A. (1992) *Science 255*, 306–312.

Dinarello, C. A. (1991) *Blood 77*, 1627–1652.

Eisenberg, S. P., Brewer, M. T., Verderber, E., Heimdal, P., Brandhuber, B. J., & Thompson, R. C. (1991) *Proc. Natl. Acad. Sci. U.S.A. 88*, 5232–5236.

Finzel, B. C., Clancy, L. L., Holland, D. R., Muchmore, S. W., Watenpaugh, K. D. & Einspahr, H. M. (1989) *J. Mol. Biol. 209*, 779–791.

Fitzgerald, P. M. D. (1988) *J. Appl. Crystallogr. 21*, 273–278.

Fitzgerald, P. M. D. (1991) *MERLOT—An integrated package of computer programs for the determination of crystal structures by molecular replacement— Version 2.4*, Merck Sharp & Dohme Research Laboratories, Rahway, NJ.

Gehrke, L., Jobling, S. A., Paik, L. S. K., McDonald, B., Rosenwasser, L. J., & Auron, P. E. (1990) *J. Biol. Chem. 265*, 5922–5925.

Graves, B. J., Hatada, M. H., Hendrickson, W. A., Miller, J. K., Madison, V. S. & Satow, Y. (1990) *Biochemistry 29*, 2679–2684.

Hendrickson, W. A., & Konnert, J. H. (1981) in *Biomolecular Structure, Conformation, Function and Evolution* (Srinivasan, R., Subramanian, E., & Yathindra, N., Ed.) pp 43–57, Pergamon Press, Oxford.

Huang, J. J., Newton, R. C., Horuk, R., Matthew, J. B., Covington, M., Pezzella, K., & Lin, Y. (1987) *FEBS Lett. 223*, 294–298.

INSIGHTII (1992) *Computational results obtained using software programs from Biosym Technologies of San Diego—dynamics calculations from DISCOVER and graphical display using INSIGHTII*, Biosym Technologies, San Diego, CA.

Jones, T. A. (1978) *J. Appl. Crystallogr. 11*, 268–272.

Ju, G., Labriola-Tompkins, E., Campen, C. A., Benjamin, W. R., Karas, J., Plocinski, J., Biondi, D., Kaffka, K. L., Kilian, P. L., Eisenberg, S. P., & Evans, R. J. (1991) *Proc. Natl. Acad. Sci. U.S.A. 88*, 2658–2662.

Kamogashira, T., Masui, Y., Ohmoto, Y., Hirato, T., Nagamura, K., Mizuno, K., Hong, Y.-M., Kikumoto, Y., Nakai, S., & Hirai, Y. (1988) *Biochem. Biophys. Res. Commun. 150*, 1106–1114.

Kraulis, P. J. (1991) *J. Appl. Crystallogr. 24*, 946–950.

Labriola-Tompkins, E., Chandran, C., Kaffka, K. L., Biondi, D., Graves, B. J., Hatada, M., Madison, V. S., Karas, J., Kilian, P. L., & Ju, G. (1991) *Proc. Natl. Acad. Sci. U.S.A. 88*, 11182–11186.

Laskowski, R. A., MacArthur, M. W., Moss, D. S., & Thornton, J. M. (1992) *PROCHECK v.2.0—programs to check the stereochemical quality of protein structures*, Oxford Molecular Ltd., London.

MacDonald, H. R., Wingfield, P., Schmeissner, U., Shaw, A., Clore, G. M., & Gronenborn, A. M. (1986) *FEBS Lett. 209*, 295–298.

Morris, A. L., MacArthur, M. W., Hutchinson, E. G., & Thornton, J. M. (1992) *Proteins 12*, 345–364.

Mosley, B., Dower, S. K., Gillis, S., & Cosman, D. (1987) *Proc. Natl. Acad. Sci. U.S.A. 84*, 4572–4576.

Nyburg, S. C. (1974) *Acta Crystallogr. B30*, 251–253.

Priestle, J. P., Schär, H.-P., & Grütter, M. G. (1988) *EMBO J. 7*, 339–343.

Priestle, J. P., Schär, H.-P., & Grütter, M. G. (1989) *Proc. Natl. Acad. Sci. U.S.A. 86*, 9667–9671.

Richardson, J. S. (1981) *Adv. Protein Chem. 34*, 167–339.

Simon, P. L., Kumar, V., Lillquist, J. S., Bhatnagar, P., Einstein, R., Lee, J., Porter, T., Green, D., Sathe, G., & Young, P. R. (1993) *J. Biol. Chem. 268*, 9771–9779.

Sims, J. E., March, C. J., Cosman, D., Widmer, M. B., MacDonald, H. R., McMahan, C. J., Grubin, C. E., Wignall, J. M., Jackson, J. L., Call, S. M., Friend, D., Alpert, A. R., Gillis, S., Urdal, D. L., & Dower, S. K. (1988) *Science 241*, 585–589.

Smith, G. D., Duax, W. L., Dodson, E. J., Dodson, G. G., De Graaf, R. A. G., & Reynolds, C. D. (1982) *Acta Crystallogr. B38*, 3028–3032.

Steiner, D. F., Chan, S. J., Welsh, J. M., & Kwok, S. C. M. (1985) *Annu. Rev. Genet. 19*, 463–484.

Stockman, B. J., Scahill, T. A., Roy, M., Ulrich, E. L., Strakalaitis, N. A., Brunner, D. P., Yem, A. W., & Deibel, M. R., Jr. (1992) *Biochemistry 31*, 5237–5245.

Stodola, R. K., Manion, F. J., Berman, H. M., & Wood, W. P. (1988) *DOCK: A program for the interactive display of molecules*, The Fox Chase Cancer Center, Philadelphia, PA.

Sweet, R. M., Wright, H. T., Janin, J., Chothia, C. H., & Blow, D. M. (1974) *Biochemistry 13*, 4212–4228.

Veerapandian, B. (1992) *Biophys. J. 62*, 112–115.

Veerapandian, B., Gilliland, G. L., Raag, R., Svensson, A. L., Masui, Y., Hirai, Y., & Poulos, T. L. (1992) *Proteins 12*, 10–23.

Xuong, N. H., Nielsen, C., Hamlin, R., & Anderson, D. (1985) *J. Appl. Crystallogr. 18*, 342–350.

Yamayoshi, M., Ohue, M., Kawashima, H., Kotani, H., Iida, M., Kawata, S., & Yamada, M. (1990) *Lymphokine Res. 9*, 405–413.

Young, P. R., & Sylvester, D. (1989) *Protein Eng. 2*, 545–551.